Environmental Science Nano

ROYAL SOCIETY OF CHEMISTRY

PAPER

View Article Online
View Journal | View Issue

Cite this: *Environ. Sci.: Nano*, 2023, 10, 2399

Metallic functionalization of magnetic nanoparticles enhances the selective removal of glyphosate, AMPA, and glufosinate from surface water†

Raghav Dogra, ‡[a] Marco Roverso, ‡[a] Giuseppe Di Bernardo, [a] Alessandra Zanut, [a] Fazel A. Monikh, [ab] Silvia Pettenuzzo, [ac] Paolo Pastore [a] and Sara Bogialli *[a]

Glyphosate (GLY) is the most used herbicide worldwide, raising concerns due to its toxicity and mobility in water. The concurrent spread of similar herbicides, *i.e.*, glufosinate (GLUF) and aminomethylphosphonic acid (AMPA, a metabolite of GLY), also causes a serious concern to the environment. The application of magnetic nanoparticles (MNPs) gained wide attention as a promising approach for the environmental remediation of GLY. However, the fast agglomeration, low removal efficiency, and saturation of MNPs by non-target chemicals remain a challenge. Herein, we used polydopamine as a coating agent followed by functionalization with different metal ions, *i.e.* Ti(IV), Zr(IV), and Cu(II), for selective removal of GLY, AMPA, and GLUF from deionised water in laboratory trials. Finally, we tested the performance of MNPs in surface waters contaminated with GLY at 0.17 ± 0.02 μg L^{-1}. The GLY removal efficiency (RE, %) of MNPs was optimized by using different GLY to MNP ratios and incubation times, in the presence of GLY-analogues and competitive species, *i.e.*, phosphates. The results indicate that all metallic functionalized MNPs are more stable toward aggregation and effective in removing GLY than bare MNPs, up to 150 μg L^{-1}. The optimal ratio was 500 μg_{GLY} g_{MNPs}^{-1} (50 μg GLY to 100 mg MNP), with RE > 80%. MNPs functionalized with Ti(IV) and Zr(IV) performed more efficiently than MNPs functionalized with Cu(II), reaching an RE of 99.9% after a incubation time of 15 min. The presence of Ti(IV) and Zr(IV) in the MNPs increased the selectivity of the particles toward GLY and GLY analogues that can be removed with similar efficiency, and prevented competition with phosphates at much higher concentrations (1000 μg L^{-1}). Finally, GLY analogues can be easily re-eluted with ammonia, and the functionalized MNPs can be efficiently re-used up to four cycles. The use of metal-functionalized MNPs is a promising approach for the removal of target pollutants from contaminated water.

Received 26th February 2023,
Accepted 12th July 2023

DOI: 10.1039/d3en00129f

rsc.li/es-nano

Environmental significance

This research paper describes some main issues that, in our opinion, are relevant for the basic knowledge in the field of nanomaterials applied to the environment: 1) functionalization of nanomaterials with polydopamine and different metals can be tuned for the selective adsorption of target compounds, *e.g.* emerging contaminants; 2) the developed materials are stable, more efficient and faster than both bare and other functionalised nanoparticles; 3) the results demonstrated that they are able to remove glyphosate directly from real surface water without any other treatment and interference with other more abundant species; 4) these materials were able to remove simultaneously glyphosate and related herbicides (AMPA and glufosinate) with very good performance and selectivity; 5) the re-elution is achievable with a non-organic solvent (*i.e.* ammonia) and the material is reusable for at least four cycles.

[a] *Department of Chemical Sciences, University of Padova, via Marzolo 1, 35131 Padova, Italy. E-mail: sara.bogialli@unipd.it; Fax: +39 049 8275207; Tel: +39 049 8275207*
[b] *Institute for Nanomaterials, Advanced Technologies and Innovation, Technical University of Liberec, Bendlova 1409/7, 460 01, Liberec, Czech Republic*
[c] *Center Agriculture Food Environment (C3A), University of Trento, IT38098 San Michele all'Adige, Italy*

† Electronic supplementary information (ESI) available. See DOI: https://doi.org/10.1039/d3en00129f

‡ R. D. and M. R. contributed equally to this work.

1. Introduction

Glyphosate (GLY) [(*N*-phosphonomethyl)glycine] is a broad spectrum nonselective herbicide, which has emerged as one of the most controversial and debated authorised pesticides in recent years.[1,2] Cases of severe environmental contamination have already been reported around the world

for GLY and its analogues/metabolites such as glufosinate (GLUF) and aminomethylphosphonic acid (AMPA). For example, Silva *et al.*[3] reported the presence of GLY and/or AMPA, its main metabolite, in 45% of the top soils originating from eleven countries and six crop systems in the European Union (EU), with a maximum concentration of 2 mg kg^{-1}. Suciu *et al.*[4] reported that the levels of ammonium GLY, AMPA, and GLUF in the groundwater of Hilly Vineyards located in the northwest of Italy are higher than the permissible concentration limit (0.1 μg L^{-1}) reported by the European Water Framework Directive as annual average environmental quality standards (AA-EQS).[5] Freshwater bodies in Florida, USA (4.74 μg L^{-1}),[6] and Melbourne, Australia (1.8 μg L^{-1})[7] have been identified as heavily contaminated with GLY. Potential negative health and environmental effects of GLY have also been reported in relation to its manufacture, transportation, and application.[8] The European Chemical Agency (ECHA) classifies GLY as toxic to aquatic life with long-lasting effects.[9] Additionally, Glyphosate's approval for use in the EU extends until December 15, 2023.[10] This highlights the importance of removing these chemicals from the environment.

Biological treatment,[11] advanced oxidation, membrane separation, and adsorption are some of the techniques proposed and developed to remediate contaminated environments with GLY.[12] In particular, adsorption stands out as the most promising remediation technique due to its ease of application, simplicity in design, economical nature, and the possibility of achieving high removal efficiency.[13] For example, numerous adsorbents can be suitably engineered for regeneration and feasible reuse in multiple adsorption cycles, leading to a notable reduction in operational cost.[14,15] Some of the adsorbent materials proposed for GLY are biochar, double laminar hydroxide (Mg–Al)[16] or metal oxides (TiO_2),[17] and magnetic nanoparticles (MNPs),[18] for example, trimethyl chitosan–silica hybrid functionalised iron oxide (NPs)[19] and reduced graphene oxide (rGO).[20] These materials exhibit different drawbacks, such as slow adsorption time,[21–23] ineffectiveness against high concentrations of contaminants,[18] lack of feasibility in implementation on a large scale and low recovery[21,22] and recyclability.[20,23] Therefore, an adsorbent material overcoming some of these disadvantages can move the adsorption treatment beyond the state of the art.

Iron oxide MNPs have been the subject of many studies in the last two decades to develop a sustainable and efficient nanobased adsorbent for environmental remediation.[24] Considerable progress has already been made in understanding the suitability of MNPs to act as an *in situ* sorbent for chemicals in different environmental compartments.[25–27] However, iron oxide MNPs have some challenges, *e.g.*, susceptibility to agglomeration upon application. Surface modification with polymers is often proposed to solve this drawback. Among these, polydopamine (PDA) is environmentally friendly and cost-efficient, and can also serve as a platform for supporting further functionalities of the particles of interest *e.g.*, for improvement in remediation capacity.[28]

In recent years, MNP functionalization with metals such as titanium (Ti) and zirconium (Zr) has gained increasing attention.[29,30] The presence of these metals on MNPs leads to a selective enrichment of phosphate-containing compounds *e.g.*, phosphopeptides and GLY.[29,31–33] At near neutral pH, the deprotonated phosphonate group of GLY is prone to strong coordination with transition metal ions.[34] Considering these, Dong *et al.*[33] developed a new efficient magnetic solid phase extraction method using PDA coated MNPs functionalized with Ti(IV) ions for selective enrichment of GLY and AMPA from river water. However, in this study, evaluation was limited to the use of this material for preconcentration of GLY and AMPA before analysis. Furthermore, it is well known that GLY binds strongly to copper ions (Cu^{2+}).[35] Nevertheless, to our knowledge, the influence of Ti, Zr and Cu cations on the capacity of MNPs in the adsorption of GLY has not yet been extensively evaluated.

The objective of this study is to develop nano-based composites of MNP@pDA@M^+, functionalized with different metals (M^+), namely Ti^{4+}, Zr^{4+} and Cu^{2+} (MNP@pDA@Ti^{4+}, MNP@pDA@Zr^{4+}, and MNP@pDA@Cu^{2+}), for the efficient and selective adsorption of GLY, AMPA, and GLUF from water. Accordingly, we first synthesize, stabilize, and functionalize MNP@pDA@M^+. Then, we comprehensively characterize them in terms of their physical and chemical properties by various spectroscopic techniques to ensure that the particles are stable against any agglomeration and transformation, such as dissolution. Then, we tested the adsorption capabilities of MNP@pDA@M^+ in ultrapure water spiked with various analyte concentrations and competitive species. After optimization of the materials, we finally tested their capacities in real GLY contaminated surface water.

2. Materials and methods

2.1 Materials and reagents

Analytical standards of GLY (*N*-(phosphonomethyl)glycine, ≥98%), glufosinate-ammonium (GLUF, 2-amino-4-(hydroxymethylphosphinyl)butyric acid ammonium salt, ≥98%), and aminomethylphosphonic acid (AMPA, 99%) were purchased from Merck. Ferric chloride hexahydrate ($FeCl_3{\cdot}6H_2O$, 97%), ferrous sulfate heptahydrate ($FeSO_4{\cdot}7H_2O$, ≥99%), Trizma® hydrochloride (TRIS HCl, tris(hydroxymethyl)aminomethane hydrochloride, ≥99%), dopamine hydrochloride (3,4-dihydroxyphenethylamine hydrochloride, 98%), titanium(IV) oxysulfate (titanyl sulfate, ≥29% Ti as TiO_2), cupric sulfate pentahydrate ($CuSO_4{\cdot}5H_2O$, ≥98%), ammonium hydroxide (NH_4OH, 28–30% NH_3), hydrochloric acid (HCl, 37%), nitric acid (69%), and formic acid (FA, ≥98%), were also obtained from Merck and used without further purification. Zirconyl chloride octahydrate ($ZrOCl_2{\cdot}8H_2O$, 98%), acetonitrile (ACN, 99.9% LC/MS grade), methanol (MeOH, 99.9% HPLC plus) and ethanol (EtOH, 99.9% HPLC plus) were supplied by Carlo Erba, Val-de-Reuill, France. Potassium hydroxide (KOH, AR grade) was supplied by Fluka Chemie AG, Buchs, Switzerland, while sodium hydroxide (NaOH, AR grade) was acquired from BDH Laboratories, Poole, Dorset,

England. Ultrapure-grade water was produced using Pure-Lab Option Q apparatus from Elga LabWater, High Wycombe, UK. Ultrapure water, purified to 18.2 MΩ cm, was obtained using a Purelab Chorus 1 system from Veolia Water Solutions and Technologies (Saint-Maurice, France).

2.2 Preparation of iron oxide MNPs

The Fe_3O_4 MNPs were synthesized by a co-precipitation method previously reported by Wang *et al.*[36] with slight modifications. Briefly, 5.2 g of $FeCl_3{\cdot}6H_2O$ and 2.8 g of $FeSO_4{\cdot}7H_2O$ [stoichiometric ratio Fe(III)/Fe(II) was 2 : 1] were dissolved in 25 mL of 0.41 mol L^{-1} HCl solution. The resulting Fe(III)/Fe(II) solution was added dropwise to the beaker containing 250 mL of 1.5 mol L^{-1} NaOH solution maintained at 80–85 °C with vigorous stirring and under an N_2 flow. The reaction mixture was stirred for another 30 minutes after the complete addition of the Fe(III)/Fe(II) solution while keeping the temperature constant at 83 °C. The bare MNPs, obtained as black precipitates, were subsequently separated from the liquid using a powerful neodymium magnet and washed three times with excess ultrapure water to remove the unreacted starting material, until reaching a neutral pH. Finally, the bare MNPs were dried overnight under vacuum and stored in a glass vial under inert conditions (Fig. 1a).

2.3 Preparation of iron oxide MNP@pDA@M^+

Synthesized MNPs were coated with pDA and functionalized with different metal ions (*i.e.* Ti(IV), Zr(IV), Cu(II)) (Fig. 1a). Accordingly, bare MNPs were dispersed in a 15 mmol L^{-1} dopamine solution prepared in 100 mM Tris-HCl buffer at pH 8.3 (100 mL) using ultrasonication for 1 min, obtaining an MNP final concentration of 2.75 g L^{-1}. Polymerization was carried out under constant magnetic stirring at 850 rpm for 6 h at room temperature. Finally, the obtained MNP@pDA was washed six times with 20 mL of acetonitrile : H_2O [50 : 50 (v/v)] to remove unreacted dopamine. MNP@pDA was then washed with 20 mL acetonitrile and dried under vacuum overnight.[37] For the metal functionalization, MNP@pDA was mixed with 20 mL of 100 mM aqueous solution of the selected metal salt ($TiOSO_4$/$ZrOCl_2{\cdot}8H_2O$/$CuSO_4{\cdot}5H_2O$). The mixtures were stirred for 2 h at room temperature and washed several times with 0.1% (v/v) formic acid. The synthesized MNP@pDA@M^+ samples were then stored in 200 μL of 0.1% formic acid at 4 °C until use.[31]

2.4 Characterization of MNPs

The particle characterization was performed by Fourier transform-infrared (FT-IR, Bruker TENSOR 27 spectrometer, Germany) and Energy Dispersive X-ray Spectroscopy (EDX, IXRF Systems 500, USA) to determine the functional group and elemental composition of the particles, respectively. The size distribution and morphology of the particles were determined using dynamic light scattering analysis (DLS, Malvern Zetasizer Nano, UK), transmission electron microscopy (TEM, JEOL JEM-2100 Plus TEM, USA), and X-ray diffraction analysis (XRD, PANalytical X'Pert-3 MRD diffractometer from PANalytical, UK). The elemental composition was obtained by inductively coupled plasma mass spectrometry (ICP-MS) using an Agilent Technologies 7700x ICP-MS system (Agilent Technologies International Japan, Ltd., Tokyo, Japan). All details are reported and discussed in the ESI† (Section 1, Tables S1–S3, and Fig. S1–S3).

2.5 Quantification of GLY, AMPA and GLUF

The GLY, AMPA and GLUF concentrations were determined using ion chromatography (Dionex ICS-6000, Thermo Fisher

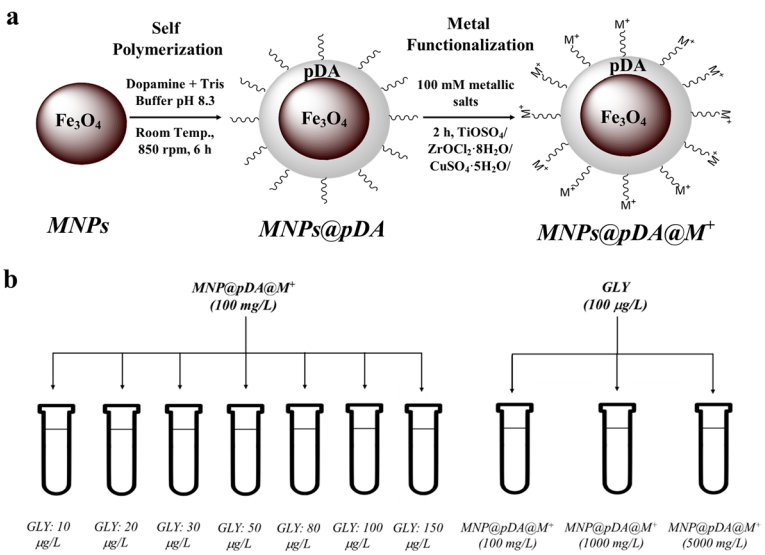

Fig. 1 a) Schematic representation of the chemically coated and functionalized MNP@pDA@M^+. b) Preparation of test solutions with different ratios of GLY to MNPs.

Scientific, Waltham, MA, USA) coupled with a Q Exactive™ hybrid quadrupole-Orbitrap™ mass spectrometer (Thermo Scientific, Waltham, MA, USA) (IC-HRMS/MS). The setup for the measurement is reported in the ESI† (Section S3). The quantification of the analytes was carried out by external calibration using a seven-point calibration curve covering the range of 0.05–20 μg L^{-1} and proper sample dilution. Linearity showed an $R^2 > 0.996$ for each analyte and the detection limit was 0.02 μg L^{-1}, with a general variability of ≤4%. For the evaluation of the analyte adsorption, data were then reported as a percentage decrease of the GLY, AMPA and GLUF signals in the aqueous solution or removal efficiency (RE%) as follows:

$$\mathrm{RE\%} = \frac{(\mathrm{signal}_0 - \mathrm{signal}_t)}{\mathrm{signal}_0} \times 100 \quad (1)$$

where signal_0 is the initial signal without adsorption and signal_t is the post-adsorption signal at incubation time t.

2.6 Evaluation of MNP@pDA@M^+: capacity in the adsorption of the chemicals

A series of experiments were performed to assess the capacity of MNP@pDA@M^+ in removing GLY, AMPA and GLUF from water. An illustration of the experiment is shown in the ESI† (Fig. S4). The adsorption experiment was performed by spiking GLY alone or in a mixture with AMPA and GLUF in ultrapure water followed by the addition of MNP@pDA@M^+. After the dispersion was mixed for a certain amount of time, the particles were separated using a magnet, and the concentrations of the contaminants in the solution were measured by IC-HRMR/MS. We tested the capacity of the particles by changing different parameters, including (a) the change of the particle to GLY ratio, (b) the presence of GLY-analogues, (c) the change of the incubation time, and (d) the presence of competitive species, *i.e.*, phosphate. To evaluate the influence of the functionalization of the particles on the adsorption of GLY, we performed a preliminary test using bare particles (*i.e.*, MNPs without functionalization) and compared the results with those obtained from functionalized particles (*i.e.* MNP@pDA@Ti^{4+}, MNP@pDA@Zr^{4+}, and MNP@pDA@Cu^{2+}).

2.6.1 Effect of MNPs on the GLY ratio. As illustrated in Fig. 1b, the effect of the GLY/MNP ratio on the removal efficiency (RE%) was first tested by varying the amount of GLY (10–150 μg L^{-1}) and keeping the concentration of MNPs stable (100 mg L^{-1}) to reach the ratios of 100, 200, 300, 500, 800, 1000, and 1500 $\mu g_{GLY}\ g_{MNPs}^{-1}$. Second, we tested the effect of the GLY/MNP ratio by varying the concentration of MNPs (100–5000 mg L^{-1}) while keeping the GLY concentration (10 μg L^{-1} and 100 μg L^{-1}) stable to reach the ratios of 2, 10, and 20 $\mu g_{GLY}\ g_{MNPs}^{-1}$. The GLY range was selected to cover the levels already reported in the literature for severe GLY contamination (exceeding 10 μg L^{-1}). The solutions were prepared in ultrapure water and mixed for 15 min. The experiment was carried out separately for MNP@pDA@Ti^{4+}, MNP@pDA@Zr^{4+}, and MNP@pDA@Cu^{2+}. The removal efficiency towards GLY analogues was also tested for MNP@pDA@Ti^{4+} and MNP@pDA@Zr^{4+} in the mixture, with GLY, GLUF and AMPA within the range of 1–20 μg L^{-1} each one (10–200 $\mu g_{analyte}\ g_{NS}^{-1}$) using the same procedure as in the previous section and keeping the concentration of MNPs at 100 mg L^{-1}.

2.6.2 Effect of incubation time. Next, we optimized the incubation time for the GLY-analogues and MNPs. Consequently, GLY and MNP concentrations were kept stable at 50 μg L^{-1} and 100 mg L^{-1}, respectively. These concentrations of GLY and MNPs were selected as the optimal adsorption capacity of MNPs and GLY (500 $\mu g_{GLY}\ g_{MNPs}^{-1}$, see also sections 3.1.1). We tested the effect of incubation time on MNP@pDA@Ti^{4+}, MNP@pDA@Zr^{4+} and MNP@pDA@Cu^{2+} separately. After mixing for 0, 5, 10, 15, 30, 60, and 120 min, the concentration of the remaining GLY in the solution was measured for each time point. We also analyzed the adsorption of GLY in the presence of analogues using a mixture of GLY (20 μg L^{-1}), GLUF (20 μg L^{-1}) and AMPA (20 μg L^{-1}). The sorption experiment in this mixture was performed using 100 mg L^{-1} of MNP@pDA@Ti^{4+} or MNP@pDA@Zr^{4+}. The concentrations of GLY, GLUF and AMPA were measured over time (120 min).

2.6.3 Effect of competitive ions. Phosphate is also known to selectively bind to transition metals such as titanium,[17] and can compete with GLY on the surface of the particles when it is present in the system. To test this hypothesis, we mixed 1 mg L^{-1} of phosphate with 10 μg L^{-1} of GLY. This concentration of phosphate was used to test MNPs under critical conditions, as in Europe the maximum allowed limit of phosphates in surface water is 700 μg L^{-1}.[38,39] The sorption experiment was carried out by adding 100 mg L^{-1} of MNP@pDA@Ti^{4+} or MNP@pDA@Zr^{4+} to the mixture of MNPs and phosphate. The concentration of GLY in the system was measured after 15 min.

2.7 Test in real water samples

The remediation efficiency of MNPs was then also tested on real surface water samples. The surface water sample was provided by Publiacqua S.p.a., a water supplier that treats the Arno River (Tuscany, Italy) for drinking water purposes. The sample was contaminated by GLY, as evidenced by their internal analysis. The pH of the water was found to be 7.90 and the GLY concentration measured by us was 0.17 ± 0.02 μg L^{-1}. The content of inorganic anions was measured by IC-conductometric detection. A 10 mL aliquot was directly treated with MNP@pDA@Ti^{4+} or MNP@pDA@Zr^{4+} at a final concentration of 100 mg L^{-1}. The procedure was repeated three times. After an incubation time of 15 min, the particles were removed with an external magnet and the GLY RE% was determined by IC-HRMS/MS.

2.8 Regeneration of MNP@pDA@M^+ for reusability

To promote the re-use of the materials, we regenerate the MNPs after their application. In this study, we focused on MNP@pDA@Ti^{4+} and MNP@pDA@Zr^{4+}, which have performed

well in the adsorption of GLY. Consequently, we first use 100 mg L^{-1} of the materials to remove GLY from a solution containing 50 μg L^{-1} of GLY over 15 min of incubation time. The desorption was carried out using different basic solutions, *i.e.* KOH and NH_4OH at different concentrations (0.1–100 mM). The MNPs were then washed (3 times, 5 min each with 0.1% formic acid in MilliQ water) for reuse. Reuse capacity of the MNPs was tested by reusing the washed MNPs (*i.e.*, after desorption of GLY) for the removal of GLY. Each usage of the MNPs after washing was considered as a cycle in this study. We repeated the use and washing (GLY desorption) for 4 cycles in total for MNP@pDA@Ti^{4+} and MNP@pDA@Zr^{4+}. A similar experiment was carried out with a mixture of GLY, GLUF and AMPA using 20 μg L^{-1} of each component (200 $\mu g_{analyte}\ g_{NS}^{-1}$).

2.9 Data acquisition and analysis

Data were evaluated statistically using SigmaPlot 14. The graphs were plotted using OriginLab 2018 and Excel Microsoft 365. One-way analysis of variance, followed by Duncan's *post hoc* test, was performed to determine statistically the significant differences between treatments. To obtain the significant differences between two groups, a *t*-test was used. The $p < 0.05$ was taken as a significant cut-off. The results are reported as the mean and standard deviation of 3–5 replicate.

3. Results and discussion

3.1 Synthesis and characterization of MNPs

Ti(IV), Zr(IV), and Cu(II) metal ions are used to increase the adsorption efficiency of the nanoparticles toward GLY. These metal ions are well known to provide great affinity to GLY so that it is possible to propose new and more efficient materials for GLY remediation.[8,40–42] The detailed results of the characterization are reported in the ESI† (Section S1). FTIR characterization was employed to confirm the formation of pDA in the intermediate coating step and its presence in the final product. As shown in Fig. 2a, the FTIR analysis of the MNPs confirms the iron oxide-based core with an intense

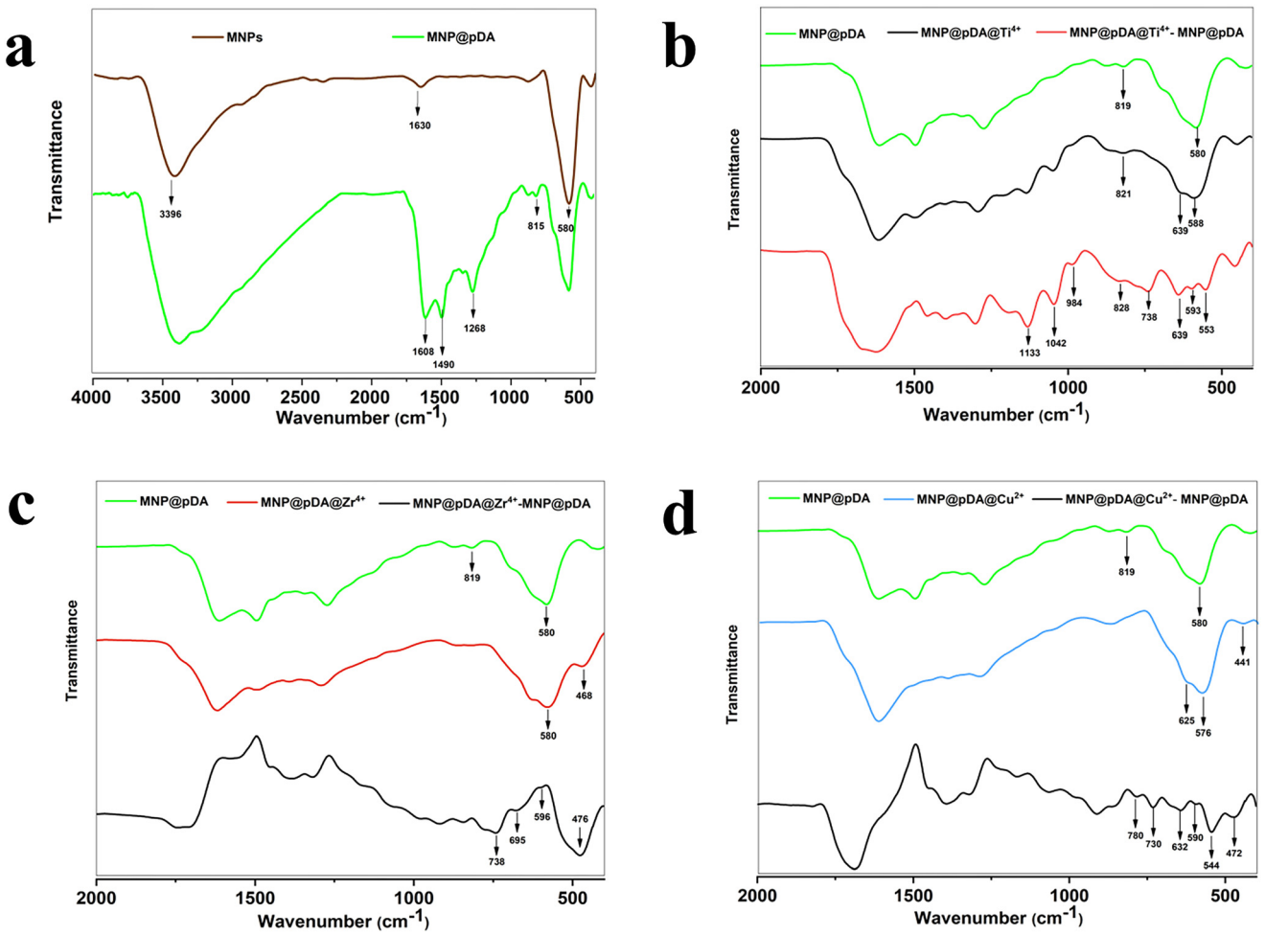

Fig. 2 FTIR spectra: (a) bare MNPs (brown) and MNP@pDA (green); (b) MNP@pDA (green), MNP@pDA@Ti^{4+} (black), and MNP@pDA@Ti^{4+} subtracting MNP@pDA (red); (c) MNP@pDA (green), MNP@pDA@Zr^{4+} (red), and MNP@pDA@Zr^{4+} subtracting MNP@pDA (black); (d) MNP@pDA (green), MNP@pDA@Cu^{2+} (blue), and MNP@pDA@Cu^{2+} subtracting MNP@pDA (black) through the KBr pellet method (1 : 100 of MNPs to KBr) at a scan rate of 64 scans per min with a resolution of 4 cm^{-1}.

signal at 570–580 cm^{-1}, attributed to the Fe–O vibration band, while the pDA coating is proved by signals in the range of 1600–1200 cm^{-1} (Table S1†). The successful functionalization of pDA with different metal ions was assessed by subtracting the FTIR spectrum of MNP@pDA from the spectra of the different MNP@pDA@M^{+}. Several characteristic signals, corresponding to those reported in the literature, were identified for Ti(IV)[43] Zr(IV)[44] and Cu(II)[45,46] as shown in Fig. 2b–d, respectively. The presence and mass loading of metals are also confirmed by ICP-MS analysis (Table S2†) showing values expressed in %w/w ranging from 0.323 of Zr to 1.890 of Ti. TEM analyses showed that the MNPs are visible as agglomerates with a quite uniform size distribution having a mean diameter of 6.1 ± 2.1 in width and 8.4 ± 2.9 nm in length (Fig. 3 and S1†), and a coating thickness of approximately 2 nm (Fig. 3e and f). The size distributions of different materials were also evaluated by DLS measurements, obtaining a mean hydrodynamic diameter of 9.6 ± 3.1 nm for bare MNPs, 11.2 ± 2.8 nm for pDA coated MNPs and 12.4 ± 2.9 nm for metal functionalized MNPs (Fig. S3†). These results demonstrate the successful synthesis of the MNPs with a narrow size distribution in the range within 10 nm of mean diameter and the further functionalization with Ti(IV), Zr(IV), and Cu(II) ions bound to the pDA coating, potentially through the catechol hydroxyl moieties.

3.2 Adsorption of GLY, AMPA and GLUF

Preliminary experiments were performed to evaluate the potential application of MNPs in the adsorption of GLY without correcting the pH values, leading to an easy application for directly treating natural waters. Experiments were subsequently extended to mixtures of GLY, GLUF, and AMPA at comparable concentrations to study both the selectivity and effectiveness of the adsorption processes toward molecules structurally very similar to GLY.

3.2.1 The influence of the GLY–MNP ratio. Important parameters influencing the ability of MNPs to adsorb analytes of interest are their actual concentration in water and the amount of material itself to be used in the procedure,[19] as it is directly correlated with the available surface area for the adsorption of the analytes. In all experiments, we performed simultaneous tests to evaluate the GLY removal efficiency (RE%) for the bare, PDA-coated and functionalized MNPs (Fig. 4 and S5†). The GLY/MNP ratio was evaluated by varying the GLY concentration (10 and 100 μg L^{-1}, Fig. 4a and 10–150 μg L^{-1}, Fig. 4b), as well as the

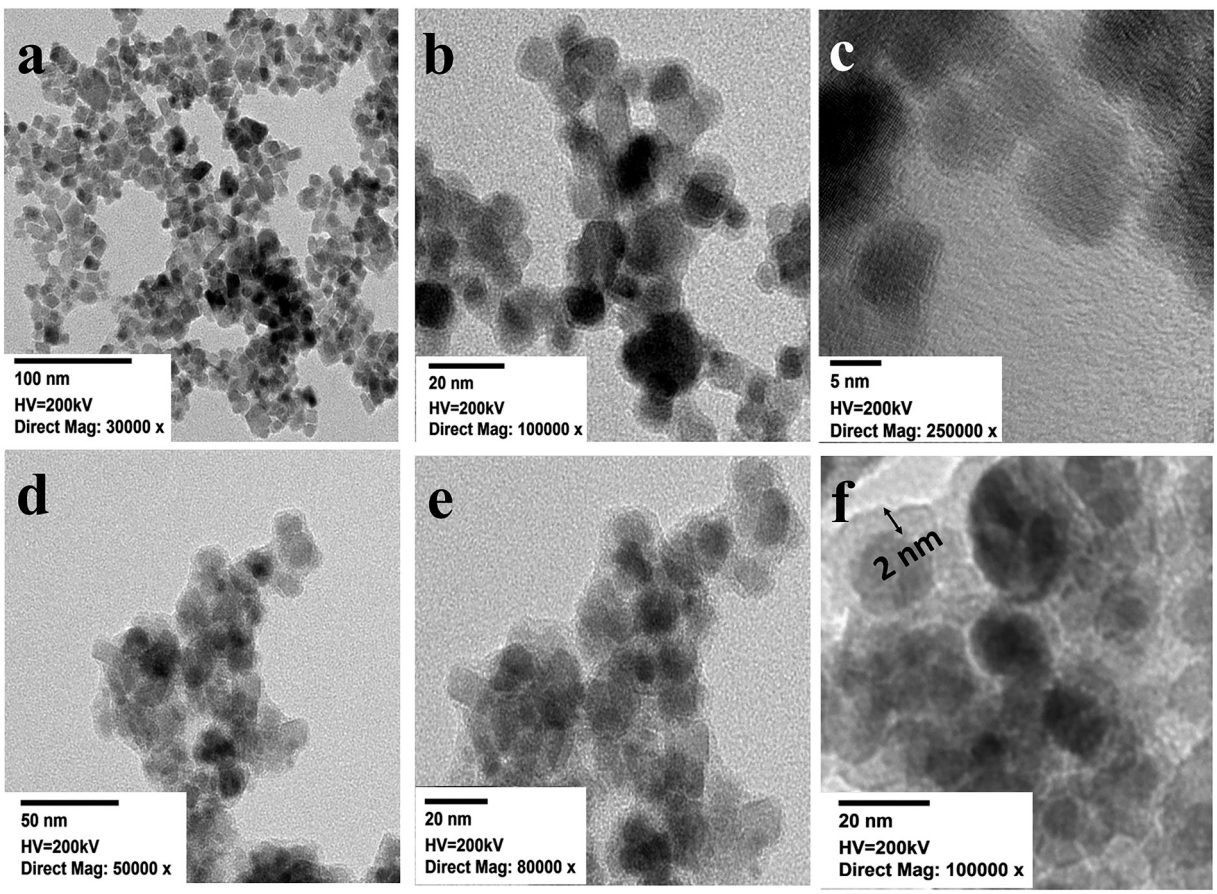

Fig. 3 MNP size and distribution measured by TEM (3a–3f). TEM images of (a) bare MNPs at 30 000×, (b) at 100 000×, and (c) at 250 000×; (d) MNP@pDA at 50 000×, (e) 80 000×, and (f) 100 000×.

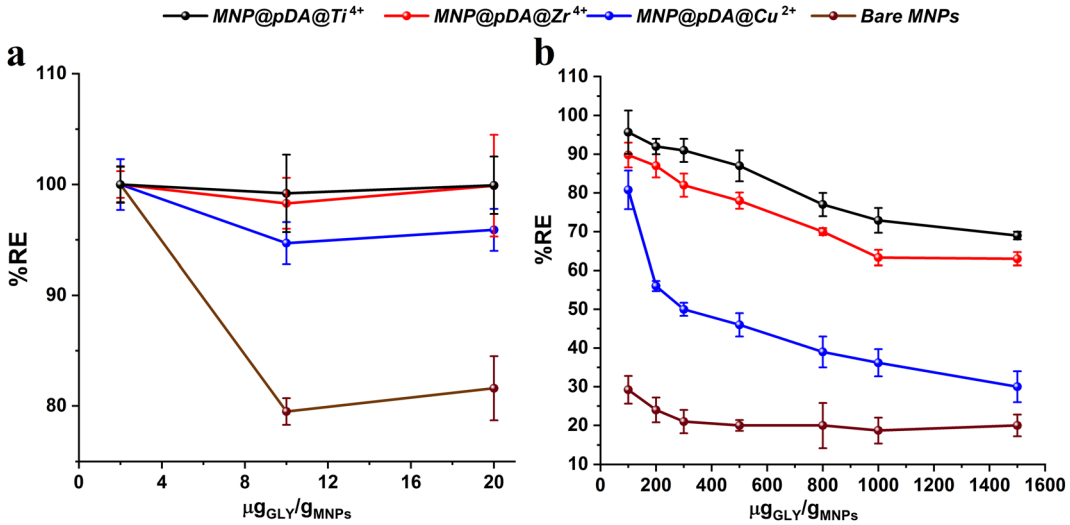

Fig. 4 Effects of the GLY/MNP ratio on the removal efficiency, at a constant incubation time (15 min) and room temperature. a) GLY removal efficiency (RE%) in the range of 2–20 $\mu g_{GLY}\ g_{MNPs}^{-1}$, by changing the concentration of MNPs (100–5000 mg L^{-1}); b) GLY removal efficiency (RE%) in the range of 100–1500 $\mu g_{GLY}\ g_{MNPs}^{-1}$ by changing the GLY concentration (10 to 150 μg L^{-1}) keeping the MNP concentration constant at 100 mg L^{-1}; data are reported as mean ± S.E.M. (n = 3).

MNP concentration (100–5000 mg L^{-1}, Fig. 4a and 100 mg L^{-1} Fig. 4b), covering a range of GLY/MNPs of 2–1500 $\mu g_{analyte}\ g_{MNPs}^{-1}$. In this set of experiments, the incubation time and temperature were kept constant (15 min, room temperature), and the results were discussed in terms of ratios of GLY/MNPs ($\mu g_{GLY}\ g_{MNPs}^{-1}$).

In the first set of experiments (Fig. 4a), the GLY concentration was kept stable at 10 and 100 μg L^{-1} while the MNP concentration changed from 100 mg L^{-1} to 5000 mg L^{-1}. The results clearly show that the functionalization with pDA doped with various metals can result in a more effective adsorption of GLY (RE% >95%) compared to the one obtained for both coated and bare MNPs, with the last ones performing well only with the lowest GLY/MNP ratio (2 $\mu g_{GLY}\ g_{MNPs}^{-1}$). For the bare MNPs, the results are consistent with the data reported by Park *et al.*[18] For the GLY/MNP ratio up to 20 $\mu g_{GLY}\ g_{MNPs}^{-1}$, MNP@pDA@$Ti^{4+}$ and MNP@pDA@Zr^{4+} were able to completely remove GLY (RE *ca.* 100%), while MNP@pDA@Cu^{2+} reached a slightly lower efficiency (RE *ca.* 95%).

Fig. 4b shows the RE% for GLY in the set of experiments in which the concentration of GLY changed while the particle concentration was kept stable, reaching a ratio comparable to those tested by other authors.[19,20,23,47–49] For all the tested ratios, MNP@pDA@Ti^{4+} showed the highest efficiency (RE% 69.3–95.7%), followed by MNP@pDA@Zr^{4+} (RE% 63.0–89.8%). MNP@pDA@Cu^{2+} was the least effective in GLY removal (RE% 29.0–80.8%). The behaviour of different tested MNP@pDA@M^{+} in the removal of GLY indicates a potential dependency on the GLY–metal binding affinity. More research is still required to obtain insight into the complex formation and to evaluate the formation constant between GLY and Ti(IV) or Zr(IV), which are currently not available, as well as AMPA and GLUF.

However, when the GLY/MNPs ratio increased from 800 to 1500 $\mu g_{GLY}\ g_{MNPs}^{-1}$, (Fig. 4a), no significant change in RE% was observed. These findings confirmed the benefit of applying pDA functionalization for MNP@pDA particles, providing a more effective adsorption than those reported elsewhere for GLY removal by using nanomaterials, and enlarging the range of application; for example, the RE% of the functionalized particles increases to 3.4 times at 1500 $\mu g_{GLY}\ g_{MNPs}^{-1}$ compared to bare particles (Fig. 4a).

For further experiments, we have selected the ratio of 500 $\mu g_{analyte}\ g_{MNPs}^{-1}$ because it was the optimal level for a very effective adsorption of GLY by the Ti(IV) and Zr(IV) functionalized MNPs.

3.2.2 Simultaneous adsorption of GLY and GLY-analogues. To understand whether MNP materials are effective in simultaneously adsorbing molecules with similar chemical and structural properties, an evaluation of MNP performance in a mixture of GLY-related compounds. *I.e.* GLY, AMPA and GLUF, was carried out. AMPA is the main microbial metabolite of GLY and is usually co-present in the environment, mainly in groundwaters.[50] GLUF is a pesticide with structural properties and efficacy similar to GLY.[51]

These molecules were tested in a range of 10 to 200 $\mu g_{analyte}\ g_{NS}^{-1}$ each, which is significant for competitive adsorption, since the highest overall ratio (600 $\mu g_{analytes}\ g_{NS}^{-1}$) slightly exceeds the optimal ratio considered (500 $\mu g_{analyte}\ g_{MNPs}^{-1}$) for GLY adsorption, where the MNPs exhibited RE% ≥80%. MNP@pDA@Ti^{4+} and MNP@pDA@Zr^{4+} were selected for this experiment, as they performed the best in previous evaluations. The results, reported in Fig. 5, indicated that also in the presence of competitive target compounds, MNP@pDA@Ti^{4+} and MNP@pDA@Zr^{4+} were able to remove a considerable amount of GLY, with RE% ranging from 91–100% and 86–100%, respectively, and indicating a comparable affinity for

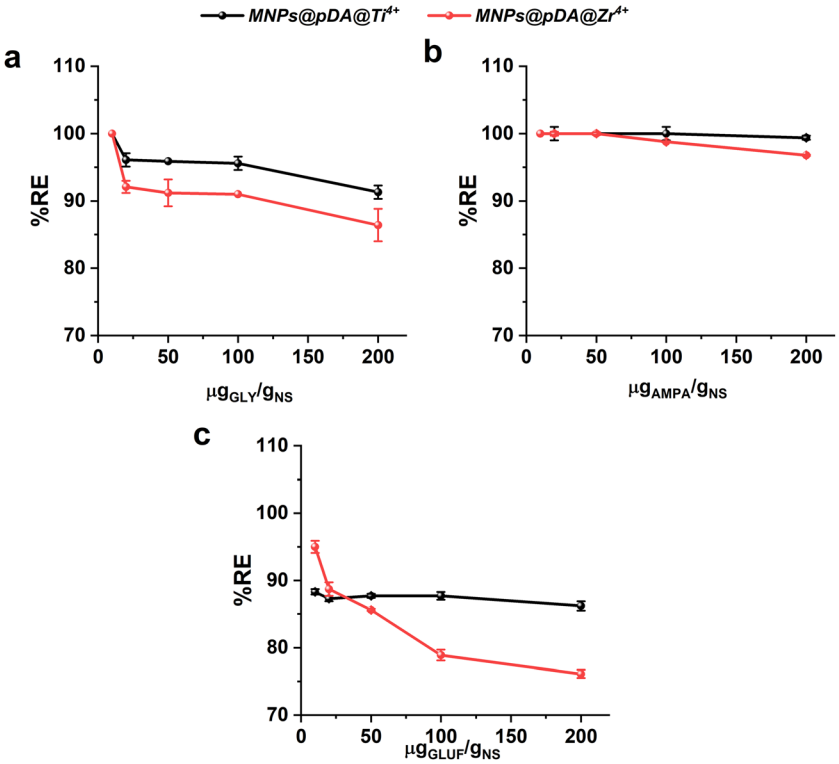

Fig. 5 Effects of the ratio $\mu g_{analyte}\ g_{MNPs}^{-1}$ on RE% of the selected target analyte in the simultaneous presence of competitive compounds at 20 μg L^{-1} each one, at room temperature with an incubation time of 15 min. Data are reported as mean ± S.E.M. (n = 3). a) GLY, b) AMPA, and c) GLUF.

GLY when the three compounds are simultaneously present in the solution (Fig. 5a).

It should be noted that the adsorption efficiency was anyway different for the specific analyte in the mixture. For AMPA, both MNPs achieved an excellent RE of 97–100% in the tested range of analyte/MNPs (Fig. 5b). Differently, for GLUF it was observed that MNP@pDA@Ti^{4+} performed better than MNP@pDA@Zr^{4+} at a value >50 $\mu g_{analyte}\ g_{MNPs}^{-1}$, ensuring RE ≥ 86% for the highest ratio compared to 76% (Fig. 5c). The overall lower adsorption of GLUF may be potentially due to the presence of an additional methyl group in the phosphonate moiety, responsible for steric hindrance and obstruction of the surface complex.[39] As previously mentioned, further studies are required to address the knowledge gap regarding the specific interaction between metals and these analytes.

3.2.3 Incubation time experiment. The RE% for GLY by different MNPs (bare MNPs, MNP@pDA@Ti^{4+}, MNP@pDA@Zr^{4+} and MNP@pDA@Cu^{2+}) was evaluated as a function of the incubation time at a ratio of 500 (50 μg L^{-1} GLY to 100 mg L^{-1} MNPs). The maximum RE% for GLY alone (Fig. 6a) was reached in 15 minutes by MNP@pDA@Ti^{4+} and MNP@pDA@Zr^{4+}, while MNP@pDA@Cu^{2+} and bare MNPs did not reach the highest RE% even within the experimental time frame of 120 min. The results of the bare MNPs (Fig. 6) were in agreement with previous studies,[18,47] which showed that the efficiency of the bare particles is lower than the efficiency of the particles functionalized with metals in removing GLY.

Fig. 6b shows the RE% for a mixture solution containing GLY + AMPA + GLUF at 20 μg L^{-1} each one over 120 min. The results showed that MNP@pDA@Ti^{4+} removed almost 100% of GLY and AMPA, and >80% for GLUF in 15 minutes. MNP@pDA@Zr^{4+} removed 100% of AMPA, and >80% of GLY and GLUF within 15 minutes. Lower performances were observed for MNP@pDA@Cu^{2+} for all chemicals and a plateau was observed only for AMPA and GLUF (within 15 minutes). Finally, bare MNPs removed 55% (RE) of GLY (alone and in the mixture) at a much longer incubation time (>120 min), but did not significantly remove AMPA (RE = 25%) and GLUF (RE = 15%). These series of experiments confirmed the best performance for MNP@pDA@Ti^{4+} followed by MNP@pDA@Zr^{4+} supporting the hypothesis of different binding affinities towards the three analytes, which can be supported by the adsorption efficiency series MNP@pDA@M^{+}–AMPA > MNP@pDA@M^{+}–GLY > MNP@pDA@M^{+}–GLUF (Fig. 6b).

These data indicate that the applied metals in the functionalization of the particles can significantly influence the time-efficiency of the particles in the removal of some pollutants despite having the same physicochemical properties. Hence, this highlights the importance of a tunable functionalization in MNPs for environmental remediation application.

We compared our results on the removal of GLY by the MNPs with the results obtained for other similar materials[18–20,23,47–49] (Table 1), since no previous studies are available for AMPA and GLUF. The MNPs presented in this work

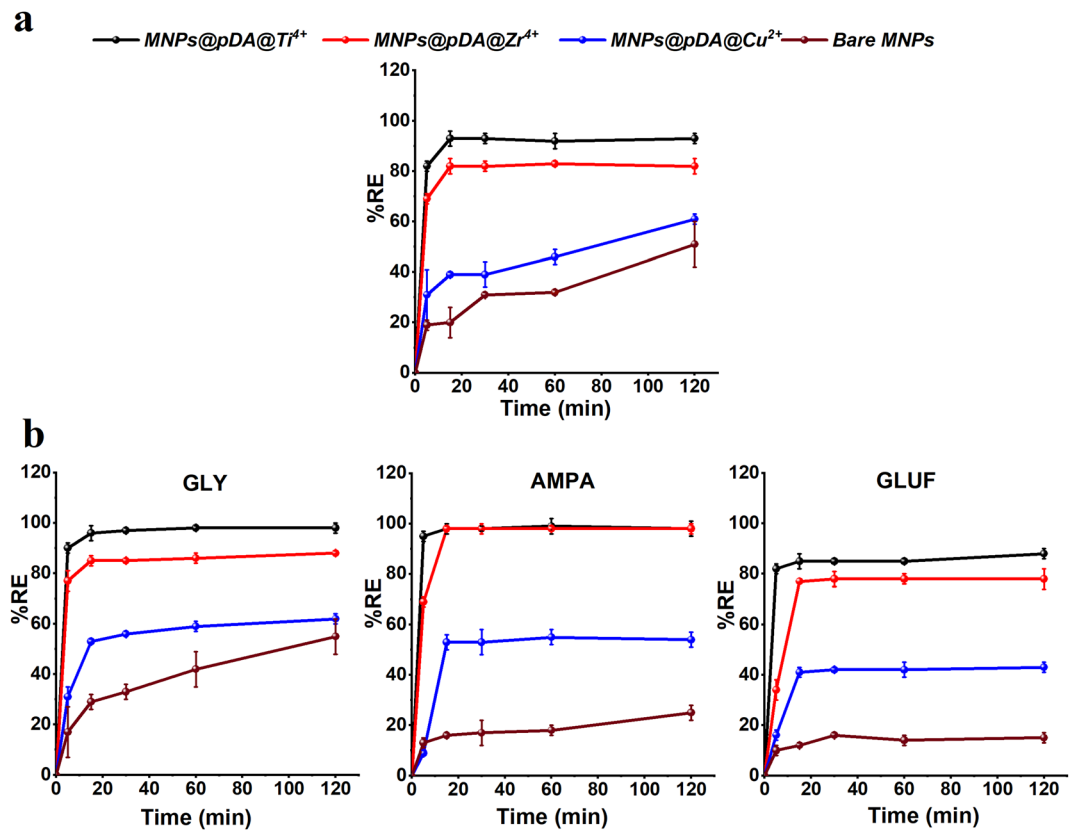

Fig. 6 Influence of incubation time on the RE% of the MNPs (100 mg L^{-1}) for a) GLY 500 μg_{GLY} g_{MNPs}^{-1}, and b) GLY 200 $\mu g_{analyte}$ g_{MNPs}^{-1} (in a mixture), AMPA 200 $\mu g_{analyte}$ g_{MNPs}^{-1} (in a mixture), and GLUF 200 $\mu g_{analyte}$ g_{MNPs}^{-1} (in a mixture), at room temperature. Data are reported as mean ± S.E.M. (n = 3).

Table 1 Comparison of equilibration time, the ratio of GLY/MNPs and the RE% of synthesized MNPs with other studies. Nr = not reported

Sorbent	μg_{GLY} g_{MNPs}^{-1}	GLY conc. used (μg L^{-1})/material used (mg L^{-1})	RE%	Size (nm)	Equilibration/incubation time (min)	Ref.
MNP@pDA@Ti^{4+}/MNP@pDA@Zr^{4+}	500	50/100	93/83	~12 nm	15	This work
Magnetite	≈0.02–10	0.05–1/100–1000	≥84	~20 nm	30	Park *et al.*[18]
Magnetite	2000	10 000/400	Nr	250 nm	120	Yang *et al.*[47]
Fe_3O_4@SiO_2/SiTMC	140 and 600	70 and 300/500	97	~98 nm	60	Soares *et al.*[19]
Mn–Fe_2O_4 graphene hybrid	2000	20 000/1000	Nr	100–400 nm	480	Yamaguchi *et al.*[23]
Reduced graphene oxide Fe_2O_4	8000	80 000/10	73	Nr	480	Li *et al.*[20]
Iron oxide NPs within SBA-15 modified with amino acid	≈350	2000/approx. 5714	Nr	15–20 nm	1440	Fiorilli *et al.*[49]
Graphene oxide decorated with α and γ-Fe_2O_3	2000	20 000/20	≥90	Nr	120	Santos *et al.*[48]

achieve the maximum RE% in less time compared to other reported materials. The MNPs developed in the current study also showed a better RE% compared to most of the previously developed materials.[18,20,23,47–49]

3.2.4 Effect of competitive analytes. Chloride, sulphate, nitrate, carbonate, and phosphate ions are well known to be commonly present in real water bodies at different concentrations. These ions could compete with the adsorption of GLY on the surface of MNPs because they are present at a higher concentration (mg L^{-1}) compared to GLY itself (<μg L^{-1}). Previous studies have already reported that chloride, sulphate and nitrate ions do not bind with Ti(IV).[17] On the other hand, phosphates exhibit a strong affinity for Ti(IV), as evident by selective adsorption of organic phosphates from environmental and biological samples, especially phosphopeptides and phosphoproteins.[52,53] Here, the competitive effect of phosphates with GLY on the surface of MNPs was tested. The GLY concentration (10 μg L^{-1}) was two orders of magnitude lower than the competitive anion (1 mg L^{-1}). As a matter of fact, an interfering competition of

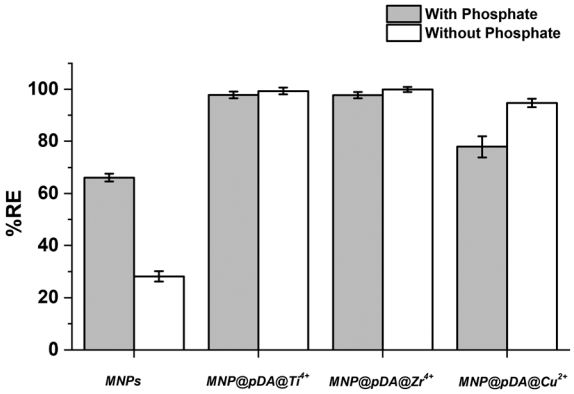

Fig. 7 Effects of phosphates (1 mg L^{-1}) as competitive ions on the adsorption of 10 μg L^{-1} GLY, at room temperature after an incubation time of 15 min. Data are reported as mean ± S.E.M. (n = 3).

phosphates shall be relevant at high concentration or high affinity of phosphate itself. Without data on the relative binding affinities, the results of the study, reported in Fig. 7, showed that phosphate, at a concentration considered quite large for the water quality, did not significantly decrease the RE% of both MNP@pDA@Ti^{4+} and MNP@pDA@Zr^{4+}. However, the RE% of MNP@pDA@Cu^{2+} and bare MNPs in the removal of GLY showed a decrease of about 15–20%. These results showed that in addition to being highly efficient in GLY removal, the developed MNP@pDA@Ti^{4+} and MNP@pDA@Zr^{4+} can also act selectively towards GLY, even in the presence of highly competitive analytes such as phosphates, also at relative higher concentration. This suggests that the developed MNPs can be potentially applied in the environment, generally consisting of matrices with complicated compositions. As a proof of principle, we tested the application of the developed MNPs in real environmental samples.

3.2.5 Application in real water samples. To evaluate the applicability of the MNPs (*i.e.* MNP@pDA@Ti^{4+} and MNP@pDA@Zr^{4+}) in real aqueous samples, an adsorption experiment was performed in a real contaminated surface water sample (collected from the Arno River, Tuscany, Italy). The sample presented 0.17 ± 0.02 μg L^{-1} of GLY (above the AA-EQS), quantified using an external calibration curve, while other residues related to GLY, AMPA and GLUF were below the LOD (0.02 μg L^{-1}). Inorganic anions in the sample were also measured, showing the presence of chlorides, nitrates, bicarbonates, and sulphates at a concentration of 29, 0.2, 50 and 420 mg L^{-1}, respectively, while phosphates were <0.1 mg L^{-1}. The results showed (Table S5†) that both MNPs (MNP@pDA@Ti^{4+} and MNP@pDA@Zr^{4+}) were able to completely remove (below the LOD) the GLY from the contaminated water. This was a challenging test, as the surface water was very complex in terms of organic and inorganic components, with the total concentration of inorganic anions three orders of magnitude higher than that of GLY. The applied tests confirmed the feasibility of applying both MNP@pDA@Ti^{4+} and MNP@pDA@Zr^{4+} in the efficient remediation of GLY-contaminated water with easy recovery from solution due to the magnetic character of the particles.

3.2.6 Testing the reusability. A critical requirement for developing a sorbent material for environmental remediation purposes is the possibility of regenerating and reuse of that material for multiple cycles. This makes the application more cost-effective and environmentally friendly.[19] Likewise, desorption properties are important to understand the molecular mechanism underlying the adsorption process and finally the extent of possible regeneration. The potential for GLY desorption was explored for the best performing MNP@pDA@Ti^{4+} using different basic solutions of NH_4OH and KOH (from a pH of approximately 10 to 13), reported in Fig. S6a.† The rationale behind this experiment was to provide a basic medium that may possibly hinder or seriously weaken the interaction between the herbicide molecule and metal ions, as already observed in the case of phospholipids.[54] The results

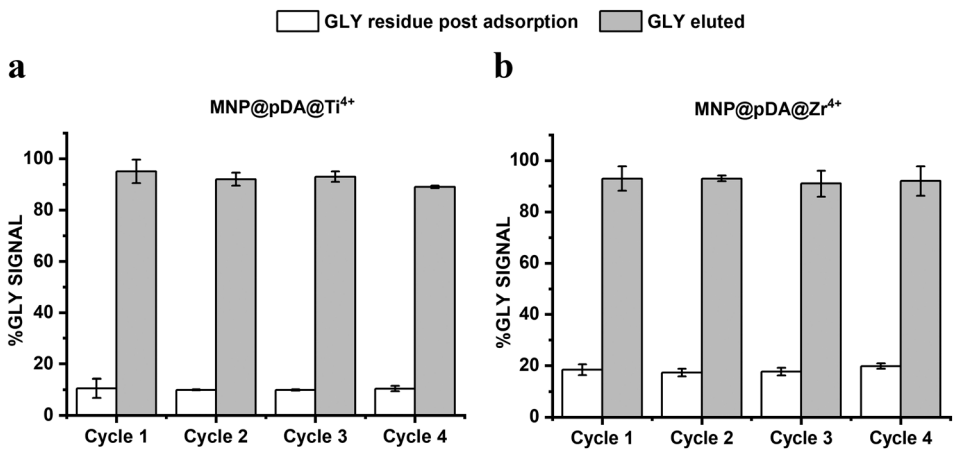

Fig. 8 Residues after adsorption (white) and desorption (grey) of GLY from the same material using 40 mM NH_4OH after multiple cycles of use at room temperature (500 $\mu g_{GLY}\ g_{MNPs}^{-1}$ of GLY and incubation time of 15 min) with (a) MNP@pDA@Ti^{4+} and (b) MNP@pDA@Zr^{4+}, as MNPs, and 40 mM NH_4OH as the eluting solvent (n = 3).

(Fig. S6†) showed that 40 mM NH_4OH was clearly the best condition among the eluting solutions tested (NH_4OH *versus* KOH) for the quantitative desorption of GLY from MNP@pDA@Ti^{4+}. From our results, it is quite clear that the basic environment is not sufficient to provide a quantitative elution of GLY, and the role of NH_4OH was found to be fundamental to achieve high GLY recoveries. Our hypothesis is that this is likely due to the displacement of GLY from the metal ion by ammonia. A higher pH value (realized even with ammonia) increases the stability constant of the metal with GLY so that even ammonia is less effective in removing it. Anyway, future studies should confirm this hypothesis. For the mixture of compounds related to GLY, the results of a single cycle of adsorption and elution (desorption) with MNP@pDA@Ti^{4+} are reported in Fig. S6b.† Different moieties resulted in almost comparable desorption results, with AMPA recording the highest desorption of 103.4 ± 8.9%, followed by GLY with 100.8 ± 2.5%, and the last being GLUF with 96.3 ± 2.9%.

Fig. 8 presents the amount of GLY after 4 consecutive adsorption and desorption cycles using MNP@pDA@Ti^{4+} and MNP@pDA@Zr^{4+}, with 40 mM NH_4OH as the desorbing agent. In the case of MNP@pDA@Ti^{4+}, an optimum elution of 95.2 ± 0.2% was observed in the first cycle of use, which did not decrease very significantly until the third cycle of use (3.2 ± 0.2%) and less than 10.4 ± 0.1% in the fourth cycle. This shows that the material is effective against GLY, robust (overall % relative standard deviation of 3.3%), and suitable for reuse using non-organic solvents. Similar results were obtained for MNP@pDA@Zr^{4+}, with 93.3 ± 0.4 to 87.1 ± 5.7% (overall 4.0% relative standard deviation) of GLY elution, consistent until the fourth cycle of use.

4. Conclusions

Magnetic nanoparticles coated with pDA and functionalized with different metals (MNP@pDA@Ti^{4+}, MNP@pDA@Zr^{4+}, and MNP@pDA@Cu^{2+}) were evaluated, for the first time, as selective nanosorbents for simultaneous remediation of GLY, AMPA and GLUF in surface water. The obtained results demonstrate that all the synthesized MNP@pDA@M^+ materials always exhibited a more efficient adsorption compared to the bare MNPs. The metal functionalization was also shown to be effective toward AMPA and GLUF, suggesting large binding affinities between MNP@pDA@M^+ and the selected compounds. MNP@pDA@Ti^{4+} and MNP@pDA@Zr^{4+} showed high removal efficiency compared to MNP@pDA@Cu^{2+}, towards a mixture solution of GLY, AMPA and GLUF. The removal of GLY within 15 min of incubation time confirms the relatively fast performance of these materials in removing GLY and its analogues, providing economically and time efficient adsorbents. Furthermore, it is possible to propose affordable regeneration of these materials, as re-elution can be carried out with a NH_4OH solution, while maintaining the removal efficiency of MNP@pDA@Ti^{4+} and MNP@pDA@Zr^{4+} for four consecutive adsorption/regeneration cycles. This might be of great importance for the removal of some chemicals that undergo fast transformation in the environment generating hazardous analytes because of, *e.g.*, degradation. However, further investigation is recommended to comprehensively address the adsorption kinetics, thermodynamics, and the specific interaction mechanisms, and therefore test the feasibility of applying the developed particles to other organic chemicals and pesticides. Finally, the application of MNP@pDA@M^+ for the removal of GLY from surface water collected from a contaminated river in Italy confirms the feasibility of applying the developed materials in real-life scenarios, in the presence of a much larger concentration of inorganic anions. With MNP@pDA@Ti^{4+} and MNP@pDA@Zr^{4+} indeed, it is possible to reach a residue of GLY below 0.1 μg L^{-1}, which meets the requirement of the European Environmental Quality Standards for surface waters. This study demonstrated that the developed materials with magnetic properties and efficient metal functionalization can be used as effective, fast, and low cost nanosorbents for the remediation of GLY in real surface water.

Author contributions

Raghav Dogra: conceptualization, investigation, methodology, formal analysis, and writing – review & editing; Marco Roverso: conceptualization, investigation, methodology, formal analysis, and writing – review & editing; Giuseppe Di Bernardo: conceptualization, investigation, methodology, and formal analysis; Alessandra Zanut: visualization and writing – review & editing; Fazel A. Monikh: visualization and writing – review & editing; Silvia Pettenuzzo: formal analysis; Paolo Pastore: supervision and review & editing; Sara Bogialli: supervision, conceptualization, writing – review & editing, and funding acquisition.

Conflicts of interest

There are no conflicts to declare.

Acknowledgements

The research project was partially supported by the Fondazione Cassa di Risparmio Padova e Rovigo (CariPaRo) and the FSE-REACT-EU, PON Ricerca e Innovazione 2014-2020 DM 1062/202, Cod: 19-G-12549-3. The authors thank Publiacqua S.p.a. for providing the surface water sample.

Notes and references

1 M. J. Davoren and R. H. Schiestl, Glyphosate-based herbicides and cancer risk: A post-IARC decision review of potential mechanisms, policy and avenues of research, *Carcinogenesis*, 2018, **39**, 1207–1215.
2 IARC, Some organophosphate insecticides and herbicides, *IARC monographs on the evaluation of carcinogenic risks to humans*, 2015, vol. 112, pp. 323–324.
3 V. Silva, L. Montanarella, A. Jones, O. Fernández-Ugalde, H. G. J. Mol and C. J. Ritsema, *et al.*, Distribution of

glyphosate and aminomethylphosphonic acid (AMPA) in agricultural topsoils of the European Union, *Sci. Total Environ.*, 2018, **621**, 1352–1359.

4 N. Suciu, E. Russo, M. Calliera, G. P. Luciani, M. Trevisan and E. Capri, Glyphosate, glufosinate ammonium, and AMPA occurrences and sources in groundwater of hilly vineyards, *Sci. Total Environ.*, 2023, **866**, 161171, Available from: **https://linkinghub.elsevier.com/retrieve/pii/S0048969722082742**.

5 European Community, Directive 2000/60/EC of the European Parliament and of the Council of 23 October 2000 establishing a framework for Community action in the field of water policy, *Official Journal of the European Parliament*, 2000, 1–82.

6 M. De María, C. Silva-Sanchez, K. J. Kroll, M. T. Walsh, M. Z. Nouri and M. E. Hunter, *et al.*, Chronic exposure to glyphosate in Florida manatee, *Environ. Int.*, 2021, **152**, 106493.

7 E. Okada, M. Allinson, M. P. Barral, B. Clarke and G. Allinson, Glyphosate and aminomethylphosphonic acid (AMPA) are commonly found in urban streams and wetlands of Melbourne, Australia, *Water Res.*, 2020, **168**, 115139.

8 K. Gandhi, S. Khan, M. Patrikar, A. Markad, N. Kumar and A. Choudhari, *et al.*, Exposure risk and environmental impacts of glyphosate: Highlights on the toxicity of herbicide co-formulants, *Environ. Challenges*, 2021, **4**, 100149.

9 *Registry of CLH intentions until outcome – ECHA*, Available from: **https://echa.europa.eu/de/registry-of-clh-intentions-until-outcome/-/dislist/details/0b0236e185e41a77**.

10 European Commission, (Text with EEA relevance) 21.6.2017, 2022, pp. 99–100.

11 L. Borella, G. Novello, M. Gasparotto, G. Renella, M. Roverso and S. Bogialli, *et al.*, Design and experimental validation of an optimized microalgae-bacteria consortium for the bioremediation of glyphosate in continuous photobioreactors, *J. Hazard. Mater.*, 2023, **441**, 129921.

12 R. Kumar, M. Qureshi, D. K. Vishwakarma, N. Al-Ansari, A. Kuriqi and A. Elbeltagi, *et al.*, A review on emerging water contaminants and the application of sustainable removal technologies, *Case Stud. Chem. Environ. Eng.*, 2022, **6**, 100219.

13 G. L. Dotto and G. McKay, Current scenario and challenges in adsorption for water treatment, *J. Environ. Chem. Eng.*, 2020, **8**(4), 103988.

14 D. P. Vargas-Delgadillo, L. Giraldo and J. C. Moreno-Piraján, Nanostructured materials for glyphosate capture—A mini-review, *Front. Sustain.*, 2022, **3**, 73.

15 P. J. Espinoza-Montero, C. Vega-Verduga, P. Alulema-Pullupaxi, L. Fernández and J. L. Paz, Technologies employed in the treatment of water contaminated with glyphosate: A review, *Molecules*, 2020, **25**(23), 5550.

16 E. Hottes, C. O. da Silva, G. F. Bauerfeldt, R. N. Castro, J. H. C. de Lima and L. P. Camargo, *et al.*, Efficient removal of glyphosate from aqueous solutions by adsorption on Mg–Al-layered double oxides: thermodynamic, kinetic, and mechanistic investigation, *Environ. Sci. Pollut. Res.*, 2022, **29**(55), 83698–83710, Available from: **https://link.springer.com/article/10.1007/s11356-022-21703-y**.

17 V. Fauvelle, T. T. Nhu-Trang, T. Feret, K. Madarassou, J. Randon and N. Mazzella, Evaluation of Titanium Dioxide as a Binding Phase for the Passive Sampling of Glyphosate and Aminomethyl Phosphonic Acid in an Aquatic Environment, *Anal. Chem.*, 2015, **87**(12), 6004–6009.

18 H. Park, A. May, L. Portilla, H. Dietrich, F. Münch and T. Rejek, *et al.*, Magnetite nanoparticles as efficient materials for removal of glyphosate from water, *Nat. Sustain.*, 2020, **3**(2), 129–135.

19 S. F. Soares, C. O. Amorim, J. S. Amaral, T. Trindade and A. L. Daniel-Da-Silva, On the efficient removal, regeneration and reuse of quaternary chitosan magnetite nanosorbents for glyphosate herbicide in water, *J. Environ. Chem. Eng.*, 2021, **9**(3), 105189.

20 Y. Li, C. Zhao, Y. Wen, Y. Wang and Y. Yang, Adsorption performance and mechanism of magnetic reduced graphene oxide in glyphosate contaminated water, *Environ. Sci. Pollut. Res.*, 2018, **25**(21), 21036–21048.

21 I. Herath, P. Kumarathilaka, M. I. Al-Wabel, A. Abduljabbar, M. Ahmad and A. R. A. Usman, *et al.*, Mechanistic modeling of glyphosate interaction with rice husk derived engineered biochar, *Microporous Mesoporous Mater.*, 2016, **225**, 280–288.

22 G. A. Dissanayake Herath, L. S. Poh and W. J. Ng, Statistical optimization of glyphosate adsorption by biochar and activated carbon with response surface methodology, *Chemosphere*, 2019, **227**, 533–540.

23 N. Ueda Yamaguchi, R. Bergamasco and S. Hamoudi, Magnetic MnFe2O4-graphene hybrid composite for efficient removal of glyphosate from water, *Chem. Eng. J.*, 2016, **295**, 391–402.

24 T. A. Aragaw, F. M. Bogale and B. A. Aragaw, Iron-based nanoparticles in wastewater treatment: A review on synthesis methods, applications, and removal mechanisms, *J. Saudi Chem. Soc.*, 2021, **25**(8), 101280.

25 N. D. Mwanza, M. E. Shigwenya, S. D. Makhanu, O. B. Victor, K. P. Gachoki and K. P. Kinoti, *et al.*, Environmental Remediation using Nanomaterial as adsorbents for Emerging Micropollutants, *Environ. Nanotechnol., Monit. Manage.*, 2023, 100789.

26 I. Ashraf, N. B. Singh and A. Agarwal, Green synthesis of iron oxide nanoparticles using Amla seed for methylene blue dye removal from water, *Mater. Today: Proc.*, 2023, **72**, 311–316.

27 M. Algamdi, A. Alshahrani and M. Alsuhybani, Chitosan grafted tetracarboxylic functionalized magnetic nanoparticles for removal of Pb(II) from an aqueous environment, *Int. J. Biol. Macromol.*, 2023, **225**, 1517–1528.

28 G. Siciliano, A. G. Monteduro, A. Turco, E. Primiceri, S. Rizzato and N. Depalo, *et al.*, Polydopamine-Coated Magnetic Iron Oxide Nanoparticles: From Design to Applications, *Nanomaterials*, 2022, **12**(7), 1145.

29 A. L. Capriotti, C. Cavaliere, F. Ferraris, V. Gianotti, M. Laus and S. Piovesana, *et al.*, New Ti-IMAC magnetic polymeric

nanoparticles for phosphopeptide enrichment from complex real samples, *Talanta*, 2018, **178**, 274–281.

30 I. Arribas Diez, I. Govender, P. Naicker, S. Stoychev, J. Jordaan and O. N. Jensen, Zirconium(IV)-IMAC Revisited: Improved Performance and Phosphoproteome Coverage by Magnetic Microparticles for Phosphopeptide Affinity Enrichment, *J. Proteome Res.*, 2021, **20**(1), 453–462.

31 S. Piovesana, A. L. Capriotti, C. Cavaliere, F. Ferraris, R. Samperi and S. Ventura, *et al.*, Phosphopeptide enrichment: Development of magnetic solid phase extraction method based on polydopamine coating and Ti4+-IMAC, *Anal. Chim. Acta*, 2016, **909**, 67–74.

32 J. Jiang, X. Sun, Y. Li, C. Deng and G. Duan, Facile synthesis of Fe3O4@PDA core-shell microspheres functionalized with various metal ions: A systematic comparison of commonly-used metal ions for IMAC enrichment, *Talanta*, 2018, **178**, 600–607.

33 Y. L. Dong, D. Q. Guo, H. Cui, X. J. Li and Y. J. He, Magnetic solid phase extraction of glyphosate and aminomethylphosphonic acid in river water using Ti 4+ −immobilized Fe 3 O 4 nanoparticles by capillary electrophoresis, *Anal. Methods*, 2015, **7**(14), 5862–5868.

34 V. Subramaniam and P. E. Hoggard, Metal complexes of glyphosate, *J. Agric. Food Chem.*, 1988, **36**(6), 1326–1329.

35 P. Yadav and F. Zelder, Detection of glyphosate with a copper(ii)-pyrocatechol violet based GlyPKit, *Anal. Methods*, 2021, **13**(38), 4354–4360.

36 Z. Wang, H. Guo, Y. Yu and N. He, Synthesis and characterization of a novel magnetic carrier with its composition of Fe3O4/carbon using hydrothermal reaction, *J. Magn. Magn. Mater.*, 2006, **302**(2), 397–404.

37 B. Socas-Rodríguez, J. Hernández-Borges, P. Salazar, M. Martín and M. Á. Rodríguez-Delgado, Core–shell polydopamine magnetic nanoparticles as sorbent in micro-dispersive solid-phase extraction for the determination of estrogenic compounds in water samples prior to high-performance liquid chromatography–mass spectrometry analysis, *J. Chromatogr. A*, 2015, **1397**, 1–10.

38 *National Primary Drinking Water Regulations*|*US EPA*, Available from: **https://www.epa.gov/ground-water-and-drinking-water/national-primary-drinking-water-regulations**.

39 *European Environment Agency, ANNEX 1 DATA SHEETS FOR SURFACE WATER QUALITY STANDARD*, 2015, Available from: **https://www.oecd.org/env/outreach/38205662.pdf**.

40 V. Fauvelle, T. T. Nhu-Trang, T. Feret, K. Madarassou, J. Randon and N. Mazzella, Evaluation of Titanium Dioxide as a Binding Phase for the Passive Sampling of Glyphosate and Aminomethyl Phosphonic Acid in an Aquatic Environment, *Anal. Chem.*, 2015, **87**(12), 6004–6009.

41 A. Pankajakshan, M. Sinha, A. A. Ojha and S. Mandal, Water-Stable Nanoscale Zirconium-Based Metal-Organic Frameworks for the Effective Removal of Glyphosate from Aqueous Media, *ACS Omega*, 2018, **3**(7), 7832–7839.

42 J. C. Diel, D. S. P. Franco, A. V. Igansi, T. R. S. Cadaval, H. A. Pereira and I. d. S. Nunes, *et al.*, Green synthesis of carbon nanotubes impregnated with metallic nanoparticles: Characterization and application in glyphosate adsorption, *Chemosphere*, 2021, **283**, 131193.

43 P. D. Moran, G. A. Bowmaker, R. P. Cooney, K. S. Finnie, J. R. Bartlett and J. L. Woolfrey, Vibrational Spectra and Molecular Association of Titanium Tetraisopropoxide, *Inorg. Chem.*, 1998, **37**(11), 2741–2748.

44 L. Khomenkova, D. Lehninger, O. Kondratenko, S. Ponomaryov, O. Gudymenko and Z. Tsybrii, *et al.*, Effect of Ge Content on the Formation of Ge Nanoclusters in Magnetron-Sputtered GeZrOx-Based Structures, *Nanoscale Res. Lett.*, 2017, **12**(1), 1–12.

45 S. Vasantharaj, S. Sathiyavimal, M. Saravanan, P. Senthilkumar, K. Gnanasekaran and M. Shanmugavel, *et al.*, Synthesis of ecofriendly copper oxide nanoparticles for fabrication over textile fabrics: Characterization of antibacterial activity and dye degradation potential, *J. Photochem. Photobiol., B*, 2019, **191**, 143–149.

46 N. B. Tanvir, O. Yurchenko, C. Wilbertz and G. Urban, Investigation of CO 2 reaction with copper oxide nanoparticles for room temperature gas sensing, *J. Mater. Chem. A*, 2016, **4**(14), 5294–5302.

47 Y. Yang, Q. Deng, W. Yan, C. Jing and Y. Zhang, Comparative study of glyphosate removal on goethite and magnetite: Adsorption and photo-degradation, *Chem. Eng. J.*, 2018, **15**(352), 581–589.

48 T. R. T. Santos, M. B. Andrade, M. F. Silva, R. Bergamasco and S. Hamoudi, Development of α- and γ-Fe2O3 decorated graphene oxides for glyphosate removal from water, *Environ. Technol.*, 2017, **40**(9), 1118–1137.

49 S. Fiorilli, L. Rivoira, G. Calì, M. Appendini, M. C. Bruzzoniti and M. Coïsson, *et al.*, Iron oxide inside SBA-15 modified with amino groups as reusable adsorbent for highly efficient removal of glyphosate from water, *Appl. Surf. Sci.*, 2017, **411**, 457–465.

50 M. Sun, H. Li and D. P. Jaisi, Degradation of glyphosate and bioavailability of phosphorus derived from glyphosate in a soil-water system, *Water Res.*, 2019, **163**, 114840.

51 M. H. Nguyen, T. D. Nguyen, M. T. Vu, H. A. Duong and H. V. Pham, Determination of Glyphosate, Glufosinate, and Their Major Metabolites in Tea Infusions by Dual-Channel Capillary Electrophoresis following Solid-Phase Extraction, *J. Anal. Methods Chem.*, 2022, **2022**, 5687025.

52 S. Tan, J. Wang, Q. Han, Q. Liang and M. Ding, A porous graphene sorbent coated with titanium(IV)-functionalized polydopamine for selective lab-in-syringe extraction of phosphoproteins and phosphopeptides, *Microchim. Acta*, 2018, **185**(7), 1–10.

53 X. H. Wang, J. L. Yu, H. D. Yang, J. Shen, H. L. Liu and J. H. Zhou, A new Ti-based IMAC nanohybrid with high hydrophilicity and enhanced absorption capacity for the selective enrichment of phosphopeptides, *J. Chromatogr., B*, 2021, **1179**, 122851.

54 F. Gao, F. Jiao, C. Xia, Y. Zhao, W. Ying and Y. Xie, *et al.*, A novel strategy for facile serum exosome isolation based on specific interactions between phospholipid bilayers and TiO2, *Chem. Sci.*, 2019, **10**(6), 1579–1588.